HHS Public Access

Author manuscript

ACS Infect Dis. Author manuscript; available in PMC 2022 June 11.

Published in final edited form as:

ACS Infect Dis. 2021 June 11; 7(6): 1558–1568. doi:10.1021/acsinfecdis.0c00899.

Changes in the V1 Loop of HIV-1 Envelope Glycoproteins Can Allosterically Modulate the Trimer Association Domain and Reduce PGT145 Sensitivity

Héctor Cervera,

Division of Infectious Diseases and International Medicine, Department of Medicine, University of Minnesota, Minneapolis, Minnesota 55455, United States

Sneha Ratnapriya,

Division of Infectious Diseases and International Medicine, Department of Medicine, University of Minnesota, Minneapolis, Minnesota 55455, United States

Angela Chov,

Division of Infectious Diseases and International Medicine, Department of Medicine, University of Minnesota, Minneapolis, Minnesota 55455, United States

Alon Herschhorn

Division of Infectious Diseases and International Medicine, Department of Medicine, University of Minnesota, Minneapolis, Minnesota 55455, United States; Microbiology, Immunology, and Cancer Biology Graduate Program, The College of Veterinary Medicine Graduate Program, and Institute for Molecular Virology, University of Minnesota, Minneapolis, Minnesota 55455, United States

Abstract

Human immunodeficiency virus (HIV-1) envelope glycoproteins (Envs) are a main focus of immunogen design and vaccine development. Broadly neutralizing antibodies (bnAbs) against HIV-1 Envs target conserved epitopes and neutralize multiple HIV-1 viral strains. Nevertheless, application of bnAbs to therapy and prevention is limited by resistant strains that are developed or preexist within the viral population. Here we studied the HIV-1_{NAB9} Envs that were isolated from a person who injects drugs and exhibits high and broad resistance to multiple bnAbs. We identified an insertion of 11 amino acids in the V1 loop that allosterically modulates HIV-1_{NAB9} sensitivity to the PGT145 bnAb, which targets the Env trimer association domain and supports high level

Corresponding Author Alon Herschhorn – Division of Infectious Diseases and International Medicine, Department of Medicine, University of Minnesota, Minneapolis, Minnesota 55455, United States; Microbiology, Immunology, and Cancer Biology Graduate Program, The College of Veterinary Medicine Graduate Program, and Institute for Molecular Virology, University of Minnesota, Minneapolis, Minnesota 55455, United States; Phone: 612-3012429; aherschh@umn.edu.

Author Contributions

A.H. designed the experiments; H.C., S.R., and A.C. performed the experiments; H.C. and A.H. analyzed the data; A.H. and H.C. wrote the paper, with all authors providing comments and suggestions.

Supporting Information

The Supporting Information is available free of charge at https://pubs.acs.org/doi/10.1021/acsinfecdis.0c00899.

Additional experimental data (PDF)

Complete contact information is available at: https://pubs.acs.org/10.1021/acsinfecdis.0c00899

The authors declare no competing financial interest.

viral infectivity. Our data provide new insights into the mechanisms of HIV-1 resistance to bnAbs and into allosteric connectivity between different HIV-1 Env domains.

Keywords

HIV-1; envelope glycoproteins; broadly neutralizing antibodies; entry inhibition

Entry of human immunodeficiency virus (HIV) into target cells is mediated by the interactions of the viral envelope glycoproteins (Envs) with the CD4 receptor and CCR5/CXCR4 coreceptor.[1–4] HIV-1 Envs are arranged in trimeric spikes on HIV-1 surface, andeach spike composes of three subunits of gp120 noncovalently associated with three subunits of membrane-anchored gp41.[5] Binding of HIV-1 Envs to the CD4 receptor triggers structural rearrangements that lead to Env transitions from a closed to more open conformations and expose the coreceptor binding site. Subsequent interactions between the coreceptor and HIV-1 Envs guide the next step on the entry pathway and lead to gp41-mediated fusion of viral and cellular membranes, facilitating HIV-1 entry into the target cell.[5–10]

HIV-1 Envs are the sole target of neutralizing antibodies. Broadly neutralizing antibodies (bnAbs) against HIV-1 Envs target conserved epitopes and neutralize multiple HIV-1 viral strains.[11–14] Accordingly, bnAbs hold promise for future therapeutic and preventive interventions and may inform efforts to develop an effective vaccine.[15] Several sites of HIV-1 Env vulnerability that are targeted by bnAbs have been identified including: (1) the CD4 binding site (CD4-bs), (2) the V1/V2 loop at the Env trimer apex, (3) the V3-glycan, (4) the silent face center of gp120, (5) the interface of gp41-gp120, (6) the gp41 fusion peptide, and (7) the membrane proximal external region (MPER) of gp41.[11] Nevertheless, the application of bnAbs to therapy and prevention is limited by rapid development of resistant strains as well as by the prevalence of HIV-1 strains with pre-existing bnAb resistance.[16,17] Especially concerning are multi-bnAb resistant strains, which can resist the combinations of different bnAbs.[16,18] Thus, it is important to study and understand the different mechanisms of HIV-1 resistance to bnAbs.

People who inject drugs (PWID) may be exposed more frequently to multiple HIV-1 infection events involving more than one HIV-1 strain and providing a productive environment for viral recombination and increased viral diversity.[19] Thus, HIV-1 strains from PWID may potentially be enriched in bnAb resistant strains. Here we studied the HIV-1_{NAB9} Envs that were isolated from a person living with HIV-1 who also injects drugs to investigate mechanisms of HIV-1 resistance to bnAbs.[18,20] Notably, HIV-1_{NAB9} Envs exhibit high and broad resistance to multiple bnAbs with complete resistance to many bnAbs that target the V1/V2 loop, V3-glycan, and gp120-gp41 interface while still sensitive to bnAbs directed against the CD4-bs and MPER gp41 (Table S1).[18] We compared the Env amino acid sequence of HIV-1_{NAB9} with those of two primary isolates and identified an insertion of 11 amino acids in the V1 loop of HIV-1_{NAB9} Env. We focused on the mechanism of resistance to bnAbs targeting the V1/V2 loop and studied the effect of the V1 insertion on HIV-1 Env function and properties. Our data support a model in which the 11

amino acid insertion in V1 loop can allosterically modulate the binding site of the V1/V2 bnAb PGT145, which targets the Env trimer association domain (TAD). These changes support high level viral infectivity.

To identify elements that are important for the resistance of HIV-1_{NAB9} Envs to multiple bnAbs, we aligned the amino acid sequence of HIV-1_{NAB9} Envs with the Env sequence of several primary isolates including: HIV-1_{BG505}, HIV-1_{JRFL}, and HIV-1_{AD8} as well as with the reference strain HXBc2 and the consensus sequence for HIV-1 clade B and M (Figure 1 and Supporting Information (SI), Figures S1 and S2). The primary reference isolates are relatively resistance to antibodies developed in people living with HIV-1 (tier 2 isolates) and have been intensively characterized in the past in numerous studies. Comparison with the reference strains identified amino acid insertions in three regions of HIV-1_{NAB9} Envs: the signal peptide (5 amino acids), V1 loop (11 amino acids), and V2 loop (2 amino acids). Interestingly, the 11 amino acid insertion in the V1 loop introduced a new N-glycosylation site on an Asn residue within the insertion and removed the NxT/S N-glycosylation motif related to potential glycosylation of Asn 142 (two residues upstream to the 11 amino acid insertion). Both changes may potentially alter of glycan pattern on NAB9 Env *in vivo*. We further focused on the long, 11 amino acid insertion, in the V1 loop, and mapped this region on an available structure of BG505 SOSIP trimer (Figure 2). Within this structure, the V1 loop is positioned next to the HIV-1 Env trimer apex and is largely exposed on the trimer surface. Moreover, the insertion is located at the tip of the V1 loop, where additional residues can be incorporated and potentially extended into the surrounding environment. This may provide a possible explanation for the ability of HIV-1 Env to tolerate such long insertion and still remain functionally active (Figure 2). Similar patterns of long V1 loop have been also observed in other studies and with clinical isolates,[22] making this flexibility a relatively common strategy of HIV-1 Env.

To evaluate the effect of the V1 insertion on HIV-1 function and sensitivity to ligands, we introduced several changes in this region. We generated four HIV Envs mutants with the complete or partial deletions of the V1 insertion resulting in Env variants with different length (Figure 2). First, we generated a mutant with a complete deletion of the 11 amino acids (designated NAB_Δ11AA), and subsequently we generated two mutants (NAB_Δ5AA and NAB_Δ6AA) to study the effects the could be mapped to the C-terminal region of the insertion (NAB_Δ5AA) or to the N-terminal region of the insertion (NAB_Δ6AA). One additional change (NAB_Δ8AA) included an unintentional additional three amino acid relative to NAB_Δ5AA, and it was included in the current study. We produced recombinant single-cycle HIV-1 viruses in 293T cells for each mutant and tested the viruses in different assays.

Pseudoviruses displaying the wild-type (WT) HIV-1_{NAB9} Envs, and the four mutants were all infectious but exhibited different levels of infectivity (Figure 3a). A complete deletion of the V1 loop insertion (NAB9_Δ11AA) reduced viral infectivity to 59% compared to WT, but deletion of only five amino acids (NAB9_Δ5AA) resulted in pseudovirus that retained WT infectivity, indicating that the five amino acids Thr-Asn-Ser-Asp-Asn were dispensable for maintaining high levels of infectivity. The N-glycosylation site motif was still present in NAB9_Δ5AA and may contribute to entry compatibility and high infectivity

as NAB9_Δ6AA, which did not contain the N-glycosylation site motif, exhibited low infectivity similar to NAB9_Δ11AA. Partial deletion of eight amino acids (NAB9_Δ8AA) significantly reduced viral infectivity to even lower levels than that observed for the complete deletion of the V1 insertion, suggesting that the Gly-Asn/Ser amino acids were beneficial only in the context of the complete insertion.

We next tested the sensitivity of the NAB9 variants to exposure to cold (Figure 3b). We and others have observed that HIV-1 Envs that frequently sample more open conformations that are associated with lower stability on ice, probably because these Envs expose elements that are more sensitive to low temperature, which are typically masked in most primary isolates.[8,23,24] We detected subtle differences between the cold sensitivity of WT NAB9 and NAB9_Δ5AA, NAB9_Δ6AA, and NAB9_Δ11AA mutants, but destabilization of none of these mutants resulted in >50% reduction of infectivity after 96 h incubation on ice. Notably, NAB9_Δ8AA, which exhibited the lowest infectivity levels, maintained this level of infectivity throughout the long incubation on ice. To study the effect of the V1 insertion on the function of HIV-1 Envs, we also studied the cell–cell fusion activity and Env sensitivity to sCD4 for the different NAB9 variants (Figure 3c, and SI, Figure S3). Interestingly, although WT NAB9 exhibited the highest viral infectivity relative to the other mutants, the cell–cell fusion activity of the WT was comparable to the virus carrying the complete 11 amino acid deletion and significantly lower than all the Envs that carried partial deletions in this region, and this difference was statistically significant for the comparison of WT with the NAB9_Δ6AA and NAB9_Δ8AA mutants (see below and SI, Table S2), the latter exhibiting lowest infectivity and highest cell–cell fusion activity among the different viruses in our study. In contrast, the sensitivity of NAB9 mutants to sCD4 neutralization was not significantly different than the sensitivity of WT NAB9.

To study the effect of the V1 insertion on bnAb sensitivity, we tested the WT NAB9 and panel of mutants against two V1/V2 directed bnAbs: PGT145 and PG9 (Figure 4). We also tested the same panel against PGT128, which is directed against the V3-glycan on HIV-1 gp120. NAB9 mutants, carrying different V1 loop changes, exhibited diverse sensitivity to the PGT145 bnAb. Deletion of eight amino acids (NAB9_Δ8AA) increased virus sensitivity to PGT145 by 6-fold compared to the WT NAB9, and similar but less profound effect was observed when the complete V1 loop insertion was deleted. Sensitivity of NAB9_Δ8AA to PGT145 was comparable (~3-fold difference) to the average of 568 different HIV-1 strains that are sensitive to PGT145. The absent of glycosylation site motif within the insertion did not contribute significantly to PGT145 sensitivity, as NAB9_Δ6AA, which lacks this motif, was as sensitive as WT NAB9. Because generation of some of the NAB9 mutants altered the glycosylation motif related to the adjacent Asn 142 (2 residue upstream of the V1 insertion), we next tested the contribution of potential glycosylation in this site to PGT145 sensitivity. We generated the NAB9 N142A mutant, which cannot be glycosylated at this position, and tested its sensitivity of PGT145. NAB9 N142A mutant was about ~4 fold more sensitive to PGT145 than the WT NAB9 (Figure 4). Thus, alteration of Asn 142-related glycosylation motif in NAB9_Δ5AA, NAB9_Δ8AA, and NAB9_Δ11AA mutants could partially explain the increased sensitivity to PGT145. In contrast, NAB9_Δ6AA that maintained the Asn 142-related glycosylation motif exhibited WT sensitivity. The resistance pattern of NAB9 to PG9 and PGT128 bnAbs was mainly unchanged among the different mutants, but the

NAB9_Δ8AA was slightly more sensitive than the WT and other variants. To visualize the different properties and compare side-by-side the specific profile of each mutant, we normalized all parameters that were measured in the different viral assays to the values of WT NAB9 and plotted the Env function and bnAb-sensitivity profile for each variant (Figure 5). This analysis allowed us to detect a pattern of differences among the diverse NAB9 variants. Overall, we detected a trend of higher PGT145 sensitivity, decreased viral infectivity, and increased cell–cell fusion activity. These changes were most profound in the activity of NAB9_Δ8AA. We also calculated statistical differences between WT NAB9 and each of the mutants using Student's *t* test. We found the most significant differences between WT and deleted mutants in the levels of viral infectivity and PGT145 sensitivity.

To gain additional structural insights into the significant effects of V1 loop changes on PGT145 sensitivity, we mapped the V1 loop insertion position on the available costructure of BG505 SOSIP in complex with PGT145 (Figure 6). Interestingly, BG505 contains a deletion in the V1 loop near the site of V1 insertion in NAB9. The binding mode of PGT145 involves penetration of a long anionic complementarity determining region of the heavy chain (HCDR3) of PGT145 into the trimer association domain (TAD) and interaction with residues from all three Env protomers.[25] Notably, the V1 loop insertion site and the binding site of PGT-145 heavy chain are far away from each other on the cocrystal structure, with about ~46 Å separating the V1 insertion site and residue Arg 100A of the PGT145 heavy chain. The long distance between the two sites makes unlikely the direct interaction between the V1 loop insertion and PGT145 or its epitope. A global change in Env conformation is also not supported by the data because: (a) the effects of V1 loop changes on Env sensitivity to cold and sCD4 are very small and not statistically significant, and (b) the changes in the V1 loop are mapped to the tip of the V1 loop, which is on the Env surface and may be extended potentially without structural clashes. Of note, despite the ability of PGT145 binding to interfere with sCD4 binding, which is likely related to steric clashes caused by prior Env binding of one ligand, the competition between the two Env ligands is not related to ability of each ligand (PGT145 or sCD4) to neutralize HIV-1 (SI, Figure S5). We conclude that the long distance between the tip of V1 loop and PGT145 binding site supports a model in which changes in the V1 loop allosterically modulate the TAD and alters PGT145 sensitivity. It is possible that direct changes in the TAD are deleterious to the trimer integrity and, thus, long-range subtle changes may provide fine-tuning to the conformation and orientation of the TAD without compromising its function. In this context, we emphasize that a partial or complete deletion of the V1 insertion resulted in only modest effects on viral sensitivity to PGT145 compared to the WT NAB9, and these effects can account only for part of the relative resistance of WT NAB9 to PGT145. The most sensitive variant among NAB9 mutants, NAB9_Δ8AA, was still 3-fold more resistant to PGT145 than the average of more than 200 primary HIV-1 isolates (Figure 4). Thus, it is likely that additional mechanisms contribute to the overall relative resistance of WT NAB9. The modest effect of V1 changes was mostly contributed by the glycosylation at residue 142 as the sensitivity of NAB9 N142A to PGT145 was comparable to the sensitivity of NAB9_Δ8AA to the PGT145 antibody. Overall, the combined effect of a change in residue 142 glycosylation and the insertion of the 11 amino acids in the V1 loop, both changes are distant from PGT145 binding site on available structures, could

partially explain the resistance of WT NAB9 to PGT145. Our finding provides insight into potential mechanism of HIV-1 resistance to PGT145 neutralization and adds to already known resistance mechanisms related to glycan shielding, changes in the target epitopes, and global conformational changes of HIV-1 Env. It is likely that all mechanisms of immune escape are important, especially as HIV-1 can potentially use multiple mechanisms to escape bnAbs. Thus, our work adds to current scientific knowledge on the different pathways of HIV-1 resistance to bnAbs.

Long gp120 V1 loop from an elite controller, which did not require antiretroviral therapy for the last 10 years, has been previously shown to confer HIV-1 resistance to neutralization by V3 glycan bnAb.[22] The original Env containing a 49-long V1 loop region was resistant to V1/V2 targeting bnAbs, but this resistance was due to the absent of Asn at position 160, which is important for V1/V2 bnAb binding. In contrast, NAB9 Envs contain residue Asn at residue 160 and changes in the V1 insertion correlate with PGT145 sensitivity. It is possible that the outcome of such changes may depend on the overall architecture of the specific Envs

Our study provides new insights into the complex biological machine of HIV-1 Envs and adds evidence to the current knowledge on allosteric interactions within HIV-1 Env. We have previously showed that the β20-β21 element of HIV-1 Env is a regulatory allosteric switch of conformational changes that are initiated by the binding of the CD4 receptor.[26] Computational studies provided evidence for long-range allosteric immune escape pathways that facilitate HIV-1 Env resistance to neutralizing antibodies.[27] Our current results support a model for allosteric control of the TAD by the V1 loop. Thus, the combination of different mechanisms, both direct and indirect, to control Env conformation and function may facilitate degenerate alternative modes of HIV-1 Envs to tolerate changes and still remain entry compatible. Understanding the flexibility and robustness of HIV-1 Env function will allow to develop new therapeutic and preventive strategies to block and prevent HIV-1 infection.

METHODS

Cell Lines.

The 293T cells were purchased from the ATCC and the TZM-bl cells were obtained from the NIH AIDS Reagent Program. Cf2Th-CD4/CCR5 target cells were generated in the laboratory of Joseph Sodroski. Cell lines were tested periodically for mycoplasma contamination.

Cell Culture.

The 293T and TZM-bl cells were grown in Dulbecco's Modified Eagle Medium (DMEM) containing 10% FBS, 100 μg/mL streptomycin, and 100 units/ml penicillin. Cf2Th-CD4/CCR5 cells were grown in the same medium supplemented with 400 μg/mL G418 and 200 μg/mL hygromycin B (both from Invitrogen, Carlsbad, CA).

Plasmid Construction.

The HIV-1_{NAB9} Env-expression plasmid was kindly provided by Peter Rusert and Alexandra Trkola. Plasmids for expression of the HIV-1_{NAB9} Env mutants were constructed by site directed mutagenesis, and correct DNA sequences were verified by Sanger sequencing.

Production of Recombinant HIV-1 Expressing Luciferase.

We produced pseudoviruses by cotransfecting 293T cells with three plasmids: HIV-1_{NAB9} Env plasmid (or HIV-1_{NAB9} Env mutants), pHIVec2.luc plasmid, and psPAX2 plasmid (catalogue no. 11348, NIH AIDS Research and Reference Reagent Program) in a ratio of 1:6:3 using calcium phosphate.[28] To increase transfection efficiency, we added a final concentration of 25 μM of chloroquine directly to the cells and incubate for 5 min prior to transfection. Then 48 h after transfection, the cell supernatant was collected and centrifuged for 5 min at 600–900*g* at 4 °C. The amount of p24 in the supernatant was measured using an in house HIV-1 p24 antigen capture assay as previously described,[29,30] and the virus-containing supernatant was frozen in single-use aliquots at −80 °C.

Viral Infection Assay.

A single-round infection assay was performed as previously described.[8,29] Briefly, HIV-1 Env ligands (antibodies and sCD4) were diluted in DMEM, and 30 μL of each tested concentration were manually dispensed in a 96-well microplates (Greiner bio-one; catalogue no. 655083). Then 30 μL containing 2 ng of p24 of viruses pseudotyped with specific Envs were then added, and after a brief incubation at room temperature, 30 μL of 1.7 × 10^5 Cf2-CD4/CCR5 target cells/mL in DMEM were added. After 48 h incubation, the medium was aspirated and cells were lysed with 30 μL of lysis buffer [(25 mM Tris, 2 mM *trans*-1,2-diaminocyclohexane-*N*,*N*,*N*′,*N*′-tetra acetic acid monohydrate, 1% Triton X-100, 10% glycerol, 2 mM dithiothreitol) titered with 15% phosphoric acid (H_3PO_4) to pH 7.8]. The activity of the firefly luciferase, which was used as a reporter protein in the system, was measured with a Centro XS^3 luminometer (Berthold Technologies, TN, USA). The effect of exposure to cold on virus infectivity was measured as previously described in detail.[29]

Cell–Cell Fusion Assay.

Cell–cell fusion was monitored as previously described.[29,31] Briefly, 500 000 293T cells in each well of 6-well plate were cotransfected with HIV Envs and HIV-1 tat expression plasmids at ratio of 1:6 (total 2 μg). After 48 h, the cells were detached with 5 mM EDTA/PBS, and 10 000 cells were added to each well of TZM-bl reporter target cells that were preseeded (10 000/well) the day before. Cells were incubated for specified time and then lysed; luciferase activity was measured as described in the viral infection assay above, and the measurements were used to evaluate the extent of fusion.

Statistical Analysis.

Statistical significance was assessed by Student's *t* test using Prism 7 program (GraphPad, San Diego, CA). Two-tailed *P* values are reported where applicable.

Calculation of Half-Maximal Inhibitory Concentration (IC_{50}).

Dose response curves of viral infection assay were fitted to the four-parameter logistic equation using Prism 7 program (GraphPad, San Diego, CA) after adding the equation to the program; IC_{50} values and the associated se are reported.[32,33] Number of experiment repeats and replicates are provided in the figure legends.

Supplementary Material

Refer to Web version on PubMed Central for supplementary material.

ACKNOWLEDGMENTS

We thank Peter Rusert and Alexandra Trkola from the Institute of Medical Virology, University of Zurich, for providing the HIV-1_{NAB9} Env-expression plasmid. We also thank the NIH AIDS Reagent Program, Division of AIDS, NIAID, NIH for providing the following anti-HIV-1 Env antibodies: PGT145, PG9, PGT128, and the psPAX2 plasmid. This work was supported by NIH/NIDA grant 1DP2DA049279–01 to A.H. Molecular graphics and analyses performed with UCSF Chimera, which is supported by NIH P41-GM103311. The content is solely the responsibility of the authors and does not necessarily represent the official views of the NIH.

REFERENCES

(1). Choe H, Farzan M, Sun Y, Sullivan N, Rollins B, Ponath PD, Wu L, Mackay CR, LaRosa G, Newman W, Gerard N, Gerard C, and Sodroski J (1996) The Beta-Chemokine Receptors CCR3 and CCR5 Facilitate Infection by Primary HIV-1 Isolates. Cell 85 (7), 1135–1148. [PubMed: 8674119]

(2). Dragic T, Litwin V, Allaway GP, Martin SR, Huang Y, Nagashima KA, Cayanan C, Maddon PJ, Koup RA, Moore JP, and Paxton WA (1996) HIV-1 Entry into CD4+ Cells Is Mediated by the Chemokine Receptor CC-CKR-5. Nature 381 (6584), 667–673. [PubMed: 8649512]

(3). Feng Y, Broder CC, Kennedy PE, and Berger EA (1996) HIV-1 Entry Cofactor: Functional CDNA Cloning of a Seven-Transmembrane, G Protein-Coupled Receptor. Science 272 (5263), 872–877. [PubMed: 8629022]

(4). Robey WG, Safai B, Oroszlan S, Arthur LO, Gonda MA, Gallo RC, and Fischinger PJ (1985) Characterization of Envelope and Core Structural Gene Products of HTLV-III with Sera from AIDS Patients. Science 228 (4699), 593–595. [PubMed: 2984774]

(5). Liu J, Bartesaghi A, Borgnia MJ, Sapiro G, and Subramaniam S (2008) Molecular Architecture of Native HIV-1 Gp120 Trimers. Nature 455 (7209), 109–113. [PubMed: 18668044]

(6). Flemming J, Wiesen L, and Herschhorn A (2018) Conformation-Dependent Interactions Between HIV-1 Envelope Glycoproteins and Broadly Neutralizing Antibodies. AIDS Res. Hum. Retroviruses 34 (9), 794–803. [PubMed: 29905080]

(7). Furuta RA, Wild CT, Weng Y, and Weiss CD (1998) Capture of an Early Fusion-Active Conformation of HIV-1 Gp41. Nat. Struct. Biol 5 (4), 276–279. [PubMed: 9546217]

(8). Herschhorn A, Ma X, Gu C, Ventura JD, Castillo-Menendez L, Melillo B, Terry DS, Smith AB, Blanchard SC, Munro JB, Mothes W, Finzi A, and Sodroski J (2016) Release of GP120 Restraints Leads to an Entry-Competent Intermediate State of the HIV-1 Envelope Glycoproteins. mBio 7 (5), 1–12.

(9). Herschhorn A, and Sodroski J (2017) An Entry-Competent Intermediate State of the HIV-1 Envelope Glycoproteins. Recept. Clin. Investig 4, e1544.

(10). Wyatt R, Kwong PD, Desjardins E, Sweet RW, Robinson J, Hendrickson WA, and Sodroski JG (1998) The Antigenic Structure of the HIV Gp120 Envelope Glycoprotein. Nature 393 (6686), 705–711. [PubMed: 9641684]

(11). Kwong PD, and Mascola JR HIV-1 Vaccines Based on Antibody Identification, B Cell Ontogeny, and Epitope Structure (2018) Immunity, pp 855–871, Cell Press. [PubMed: 29768174]

(12). Walker LM, Huber M, Doores KJ, Falkowska E, Pejchal R, Julien JP, Wang SK, Ramos A, Chan-Hui PY, Moyle M, Mitcham JL, Hammond PW, Olsen OA, Phung P, Fling S, Wong CH, Phogat S, Wrin T, Simek MD, Koff WC, Wilson IA, Burton DR, and Poignard P (2011) Broad Neutralization Coverage of HIV by Multiple Highly Potent Antibodies. Nature 477, 466–470. [PubMed: 21849977]

(13). Huang J, Kang BH, Pancera M, Lee JH, Tong T, Feng Y, Imamichi H, Georgiev IS, Chuang G-Y, Druz A, Doria-Rose NA, Laub L, Sliepen K, van Gils MJ, de la Peña AT, Derking R, Klasse P-J, Migueles SA, Bailer RT, Alam M, Pugach P, Haynes BF, Wyatt RT, Sanders RW, Binley JM, Ward AB, Mascola JR, Kwong PD, and Connors M (2014) Broad and Potent HIV-1 Neutralization by a Human Antibody That Binds the Gp41-Gp120 Interface. Nature 515 (7525), 138–142. [PubMed: 25186731]

(14). Huang J, Kang BH, Ishida E, Zhou T, Griesman T, Sheng Z, Wu F, Doria-Rose NA, Zhang B, McKee K, O'Dell S, Chuang G-Y, Druz A, Georgiev IS, Schramm CA, Zheng A, Joyce MG, Asokan M, Ransier A, Darko S, Migueles SA, Bailer RT, Louder MK, Alam SM, Parks R, Kelsoe G, Von Holle T, Haynes BF, Douek DC, Hirsch V, Seaman MS, Shapiro L, Mascola JR, Kwong PD, and Connors M (2016) Identification of a CD4-Binding-Site Antibody to HIV That Evolved Near-Pan Neutralization Breadth. Immunity 45 (5), 1108–1121. [PubMed: 27851912]

(15). Haynes BF, Burton DR, and Mascola JR (2019) Multiple Roles for HIV Broadly Neutralizing Antibodies. Sci. Transl. Med 11, eaaz2686. [PubMed: 31666399]

(16). Bar-On Y, Gruell H, Schoofs T, Pai JA, Nogueira L, Butler AL, Millard K, Lehmann C, Suárez I, Oliveira TY, Karagounis T, Cohen YZ, Wyen C, Scholten S, Handl L, Belblidia S, Dizon JP, Vehreschild JJ, Witmer-Pack M, Shimeliovich I, Jain K, Fiddike K, Seaton KE, Yates NL, Horowitz J, Gulick RM, Pfeifer N, Tomaras GD, Seaman MS, Fätkenheuer G, Caskey M, Klein F, and Nussenzweig MC (2018) Safety and Antiviral Activity of Combination HIV-1 Broadly Neutralizing Antibodies in Viremic Individuals. Nat. Med 24 (11), 1701–1707. [PubMed: 30258217]

(17). Bar KJ, Sneller MC, Harrison LJ, Justement JS, Overton ET, Petrone ME, Salantes DB, Seamon CA, Scheinfeld B, Kwan RW, Learn GH, Proschan MA, Kreider EF, Blazkova J, Bardsley M, Refsland EW, Messer M, Clarridge KE, Tustin NB, Madden PJ, Oden K, O'Dell SJ, Jarocki B, Shiakolas AR, Tressler RL, Doria-Rose NA, Bailer RT, Ledgerwood JE, Capparelli EV, Lynch RM, Graham BS, Moir S, Koup RA, Mascola JR, Hoxie JA, Fauci AS, Tebas P, and Chun T-W (2016) Effect of HIV Antibody VRC01 on Viral Rebound after Treatment Interruption. N. Engl. J. Med 375 (21), 2037–2050. [PubMed: 27959728]

(18). Rusert P, Kouyos RD, Kadelka C, Ebner H, Schanz M, Huber M, Braun DL, Hozé N, Scherrer A, Magnus C, Weber J, Uhr T, Cippa V, Thorball CW, Kuster H, Cavassini M, Bernasconi E, Hoffmann M, Calmy A, Battegay M, Rauch A, Yerly S, Aubert V, Klimkait T, Böni J, Fellay J, Regoes RR, Günthard HF, and Trkola A (2016) Determinants of HIV-1 Broadly Neutralizing Antibody Induction. Nat. Med 22, 1260–1267. [PubMed: 27668936]

(19). Bar KJ, Li H, Chamberland A, Tremblay C, Routy JP, Grayson T, Sun C, Wang S, Learn GH, Morgan CJ, Schumacher JE, Haynes BF, Keele BF, Hahn BH, and Shaw GM (2010) Wide Variation in the Multiplicity of HIV-1 Infection among Injection Drug Users. J. Virol 84 (12), 6241–6247. [PubMed: 20375173]

(20). Trkola A, Kuster H, Rusert P, Joos B, Fischer M, Leemann C, Manrique A, Huber M, Rehr M, Oxenius A, Weber R, Stiegler G, Vcelar B, Katinger H, Aceto L, and Günthard HF (2005) Delay of HIV-1 Rebound after Cessation of Antiretroviral Therapy through Passive Transfer of Human Neutralizing Antibodies. Nat. Med 11 (6), 615–622. [PubMed: 15880120]

(21). Pettersen EF, Goddard TD, Huang CC, Couch GS, Greenblatt DM, Meng EC, and Ferrin TE (2004) UCSF Chimera–a Visualization System for Exploratory Research and Analysis. J. Comput. Chem 25 (13), 1605–1612. [PubMed: 15264254]

(22). Silver ZA, Dickinson GM, Seaman MS, and Desrosiers RC (2019) A Highly Unusual V1 Region of Env in an Elite Controller of HIV Infection. J. Virol 93 (10), e00094–19. [PubMed: 30842322]

(23). Kassa A, Madani N, Schön A, Haim H, Finzi A, Xiang S-H, Wang L, Princiotto A, Pancera M, Courter J, Smith AB, Freire E, Kwong PD, and Sodroski J (2009) Transitions to and from the CD4-Bound Conformation Are Modulated by a Single-Residue Change in the Human

Immunodeficiency Virus Type 1 Gp120 Inner Domain. J. Virol 83 (17), 8364–8378. [PubMed: 19535453]

(24). Herschhorn A, Gu C, Espy N, Richard J, Finzi A, and Sodroski JG (2014) A Broad HIV-1 Inhibitor Blocks Envelope Glycoprotein Transitions Critical for Entry. Nat. Chem. Biol 10 (10), 845–852. [PubMed: 25174000]

(25). Lee JH, Andrabi R, Su CY, Yasmeen A, Julien JP, Kong L, Wu NC, McBride R, Sok D, Pauthner M, Cottrell CA, Nieusma T, Blattner C, Paulson JC, Klasse PJ, Wilson IA, Burton DR, and Ward AB (2017) A Broadly Neutralizing Antibody Targets the Dynamic HIV Envelope Trimer Apex via a Long, Rigidified, and Anionic β-Hairpin Structure. Immunity 46 (4), 690–702. [PubMed: 28423342]

(26). Herschhorn A, Gu C, Moraca F, Ma X, Farrell M, Smith AB, Pancera M, Kwong PD, Schön A, Freire E, Abrams C, Blanchard SC, Mothes W, and Sodroski JG (2017) The B20-B21 of Gp120 Is a Regulatory Switch for HIV-1 Env Conformational Transitions. Nat. Commun 8 (1), 1049. [PubMed: 29051495]

(27). Sethi A, Tian J, Derdeyn CA, Korber B, and Gnanakaran S (2013) A Mechanistic Understanding of Allosteric Immune Escape Pathways in the HIV-1 Envelope Glycoprotein. PLoS Comput. Biol 9, e1003046. [PubMed: 23696718]

(28). Jordan M, Schallhorn A, and Wurm FM (1996) Transfecting Mammalian Cells: Optimization of Critical Parameters Affecting Calcium-Phosphate Precipitate Formation. Nucleic Acids Res. 24 (4), 596–601. [PubMed: 8604299]

(29). Ratnapriya S, Chov A, and Herschhorn A (2020) A Protocol for Studying HIV-1 Envelope Glycoprotein Function. STAR Protoc 1, 100133. [PubMed: 33377027]

(30). Harris M, Ratnapriya S, Chov A, Cervera H, Block A, Gu C, Talledge N, Mansky LM, Sodroski J, and Herschhorn A (2020) Slow Receptor Binding of the Noncytopathic HIV-2UC1 Envs Is Balanced by Long-Lived Activation State and Efficient Fusion Activity. Cell Rep. 31 (10), 107749. [PubMed: 32521274]

(31). Herschhorn A, Finzi A, Jones DM, Courter JR, Sugawara A, Smith AB, and Sodroski JG (2011) An Inducible Cell-Cell Fusion System with Integrated Ability to Measure the Efficiency and Specificity of HIV-1 Entry Inhibitors. PLoS One 6, e26731. [PubMed: 22069466]

(32). Weitman M, Lerman K, Nudelman A, Major DT, Hizi A, and Herschhorn A (2011) Structure-Activity Relationship Studies of 1-(4-Chloro-2,5-Dimethoxyphenyl) −3-(3-Propoxypropyl)Thiourea, a Non-Nucleoside Reverse Transcriptase Inhibitor of Human Immunodeficiency Virus Type-1. Eur. J. Med. Chem 46 (2), 447–467. [PubMed: 21159409]

(33). Herschhorn A, Oz-Gleenberg I, and Hizi A (2008) Mechanism of Inhibition of HIV-1 Reverse Transcriptase by the Novel Broad-Range DNA Polymerase Inhibitor N-{2-[4-(Aminosulfonyl)Phenyl]Ethyl}−2-(2- Thienyl)Acetamide. Biochemistry 47 (1), 490. [PubMed: 18052256]

(34). Madeira F, Park YM, Lee J, Buso N, Gur T, Madhusoodanan N, Basutkar P, Tivey ARN, Potter SC, Finn RD, and Lopez R (2019) The EMBL-EBI Search and Sequence Analysis Tools APIs in 2019. Nucleic Acids Res. 47, W636–W641. [PubMed: 30976793]

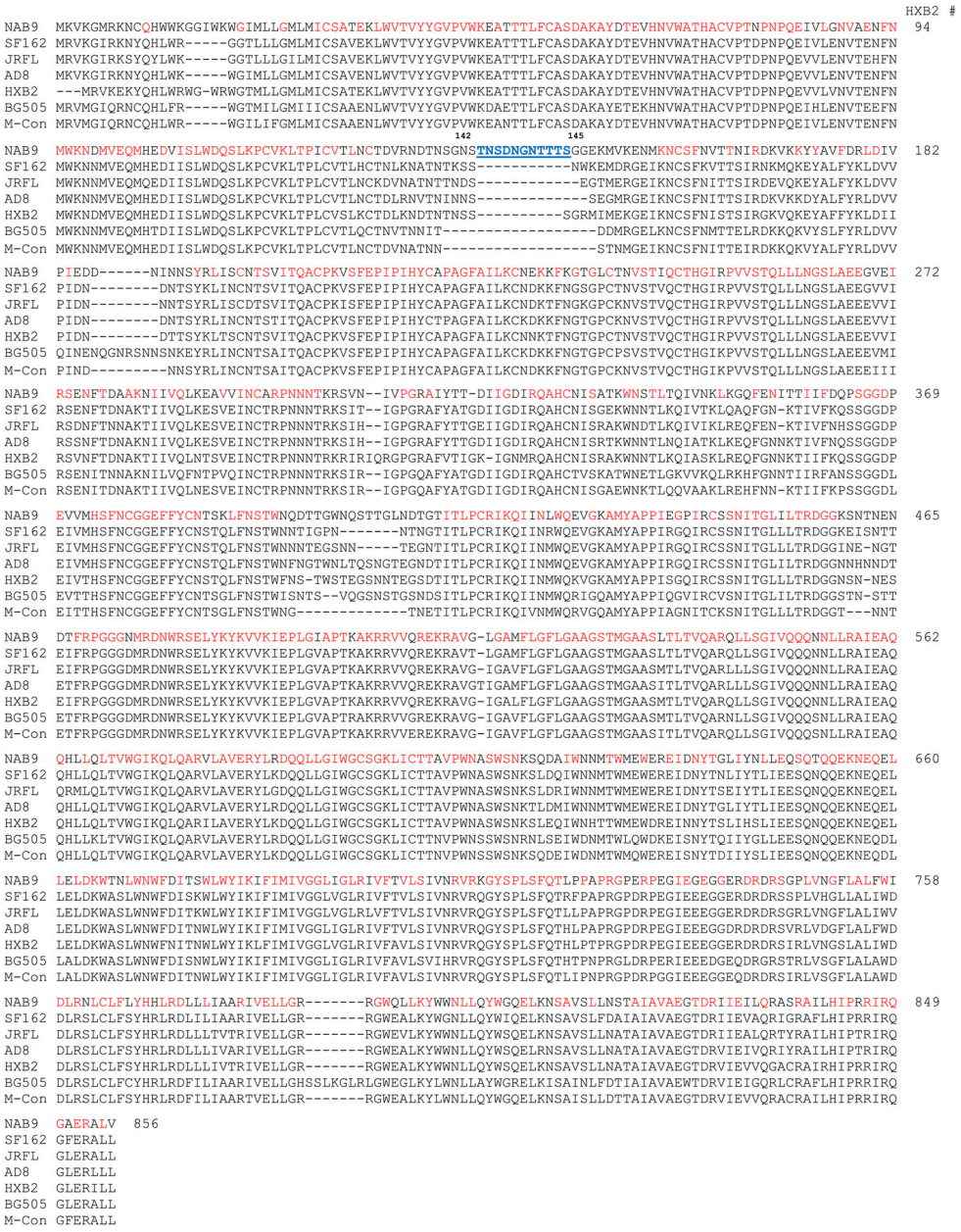

Figure 1.

Alignment of Env amino acid sequence of HIV-1_{NAB9} and other HIV-1 isolates. Amino acid sequences of HIV-1_{NAB9}, HIV-1_{SF162}, HIV-1_{JRFL}, HIV-1_{AD8}, HIV-1_{BG505}, and consensus sequence of M group (M-Con) Envs were aligned using Clustal Omega (ref 34 see SI, Figures S1 and S2); residues are numbered on the right according to the HXBc2 consensus (CATNAP program). An 11 amino acid insertion in the V1 loop of NAB9 is in light blue, and all residues in NAB9 that are identical in all sequences are in red.

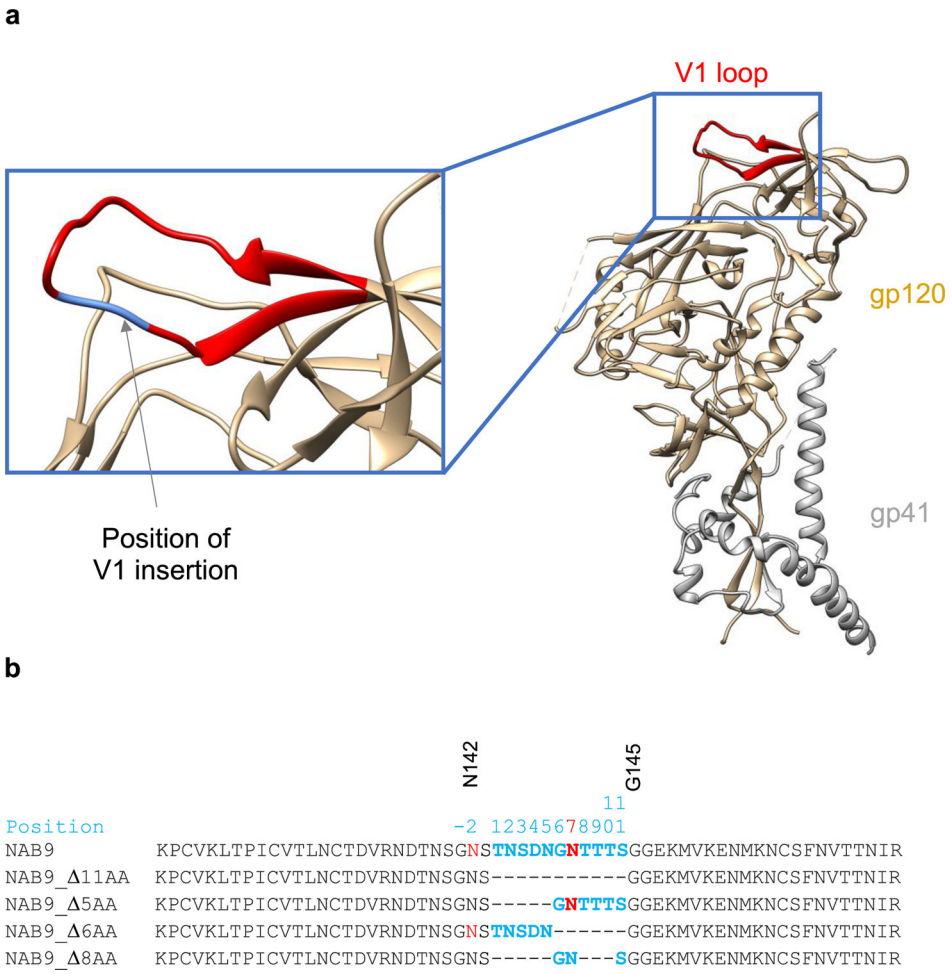

Figure 2.

Mapping the NAB9 V1 loop insertion on an available structure of BG505 SOSIP trimer. (a) (right) The BG505 SOSIP trimer structure (a single protomer) with gp120 highlighted in tan. (left) The position of the 11 amino acid insertion in the V1 loop of NAB9 were mapped on the BG505 SOSIP structure (Protein Data Base (PDB) 4TVP) and shown in light blue. The V1 loop is shown in red. Structure was visualized using the Chimera software.[21] (b) NAB9 variants. Env amino acid alignment of NAB9 wild-type (WT) and NAB9 deletion mutants generated in this study. Amino acids that are part of the 11 amino acid insertion are shown in light blue, and an Asn residue within an N-glycosylation motif is shown in red.

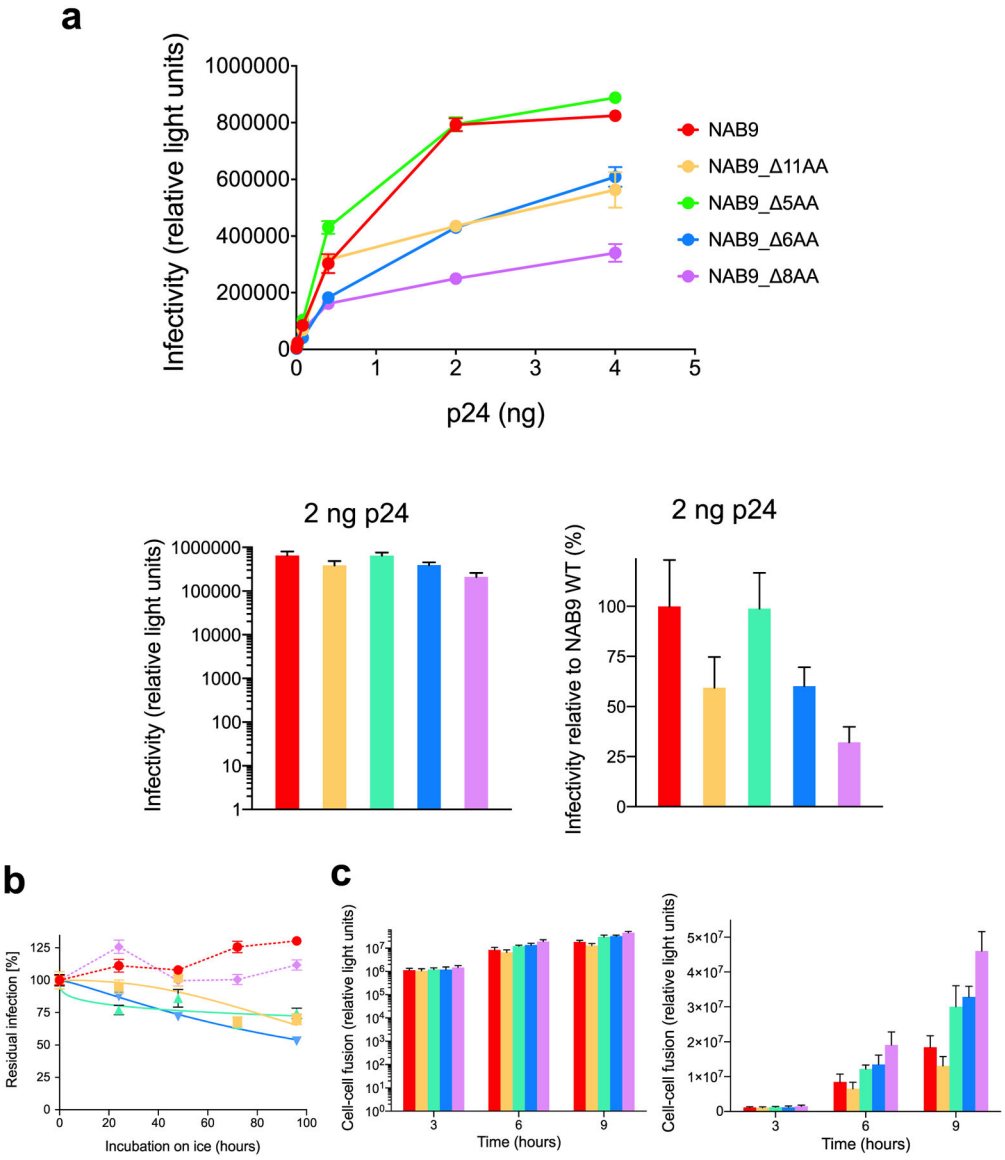

Figure 3.

HIV-1 Env function of different HIV-1_{NAB9} variants. (a) Virus infectivity. (top) Pseudoviruses displaying Envs of the different NAB9 variants were prepared in 293T cells and increasing p24 amounts for each variant were used to infect Cf2Th-CD4/CCR5 cells. Viral infectivity was evaluated by measuring the activity of the reporter protein firefly luciferase 48 h post infection. (bottom) 2 ng of p24 of each NAB9 variant was used to infect Cf2Th-CD4/CCR5 cells, and absolute values (left) or normalized to WT NAB9 values (right) were plotted for the different viruses. (b) Cold sensitivity. Pseudoviruses were exposed to cold for the specified time and then allowed to infect Cf2Th-CD4/CCR5 cells. (c) Cell–cell fusion activity was measured as described under the Methods. Results are shown on logarithmic (left) or linear (right) scales. Color codes are identical in all panels. Results represent average ± standard deviation of 5–10 measurements (derived from 2–5 independent experiments, each performed in 2–4 replicates).

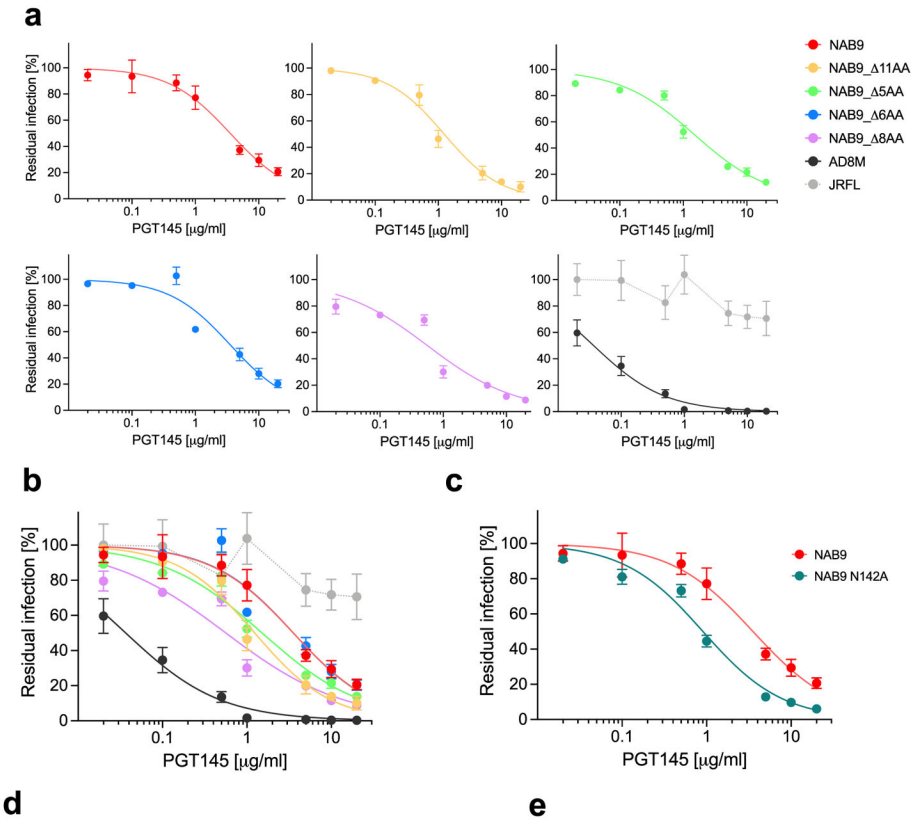

d

Virus isolate /mutant	IC_{50} bnAb (µg/ml)			
	V1-V2 loop			V3 Glycan
	PGT145	Fold change	PG9	PGT128
NAB9	3.54 ± 0.38	1	>50	>50
NAB9_Δ11AA	1.24 ± 0.20	2.9	>50	>50
NAB9_Δ5AA	1.51 ± 0.31	2.3	>50	>50
NAB9_Δ6AA	3.54 ± 0.96	1	>50	>50
NAB9_Δ8AA	0.56 ± 0.20	6.3	>50	48.58
NAB9 N142A	0.91 ± 0.16	3.9	ND	ND
AD8M (positive)	0.024 ± 0.005	NA	ND	ND
JRFL (negative)	>20	NA	ND	ND

e

Viral population sensitivity (IC_{50} bnAb µg/ml)

	V1-V2 loop		V3 Glycan
	PGT145	PG9	PGT128
Geometric mean IC_{50}*	0.17	0.19	0.06
sensitive strains**	568	418	450
resistant strains**	200	254	201

* IC_{50} of sensitive strains
** Number of strains

Figure 4.

Sensitivity of NAB9 variants to bnAbs targeting the V1/V2 loop and V3 glycan. (a) The effect of increasing concentrations of the V1/V2 bnAb PGT145 on the entry of NAB9 variants into Cf2Th-CD4/CCR5 cells was tested and the results used to plot normalized dose response curves for each NAB9 variant. AD8M was used as a positive control and JRFL as a negative control. Complete range of AD8M sensitivity is shown in SI, Figure S4 (b) Overlay of plots from (a) with the same color code. (c) Inhibition curve of NAB9 N142A and WT NAB9. (d) Half-maximal inhibitory concentrations (IC_{50s}) of PGT145, PG9, and PGT128 bnAbs for blocking the infection of NAB9 variants were calculated by nonlinear fitting of the dose response curves to the logistic (four-parameter) equation. (e) Viral population sensitivity of more than 200 HIV-1 strains expressed as geometric mean IC_{50} for the three bnAbs was retrieved from the HIV database (https://www.hiv.lanl.gov).

Results represent fitted IC_{50} ± standard error derived from the six measurements for each concentration (average of three independent experiments, each performed in duplicate).

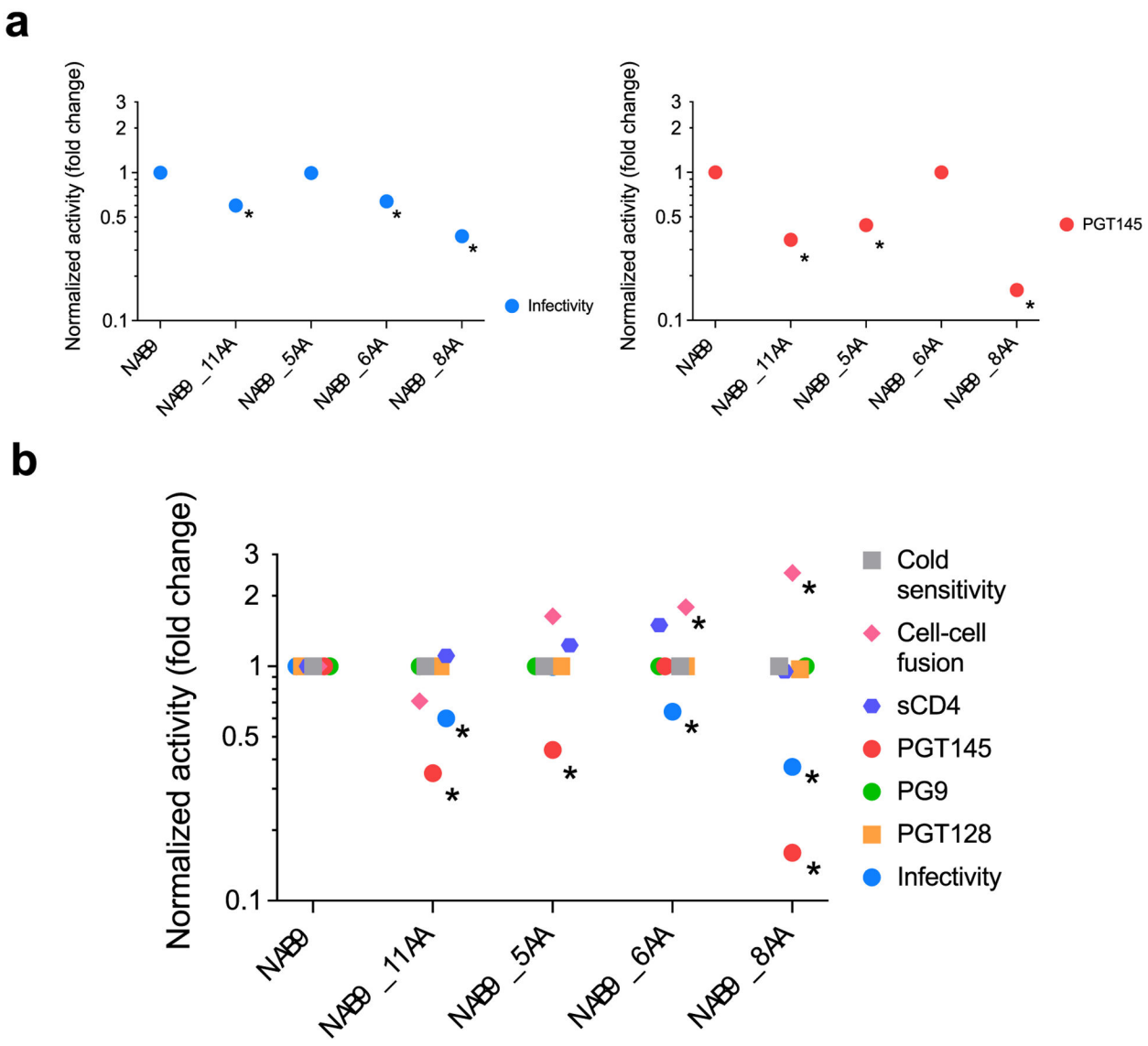

Figure 5.

Profile of HIV-1 Env function and sensitivity to different ligands of the NAB9 variants. (a) Normalized plots. Infectivity (left) and PGT145 sensitivity (right) values of NAB9 mutants normalized to wild-type NAB9 values. (b) Integration of normalized plots. IC_{50}, cell–cell fusion at 9 h, infectivity, and $t_{1/2}$ values for each NAB9 mutant were normalized to WT NAB9 values and are shown on a single scale, generating a single profile that integrates all measurements for each mutant. *Values that significantly differ from WT NAB9 values (two-tailed *P* value <0.05; Student's *t* test; exact values are shown in SI, Table S2).

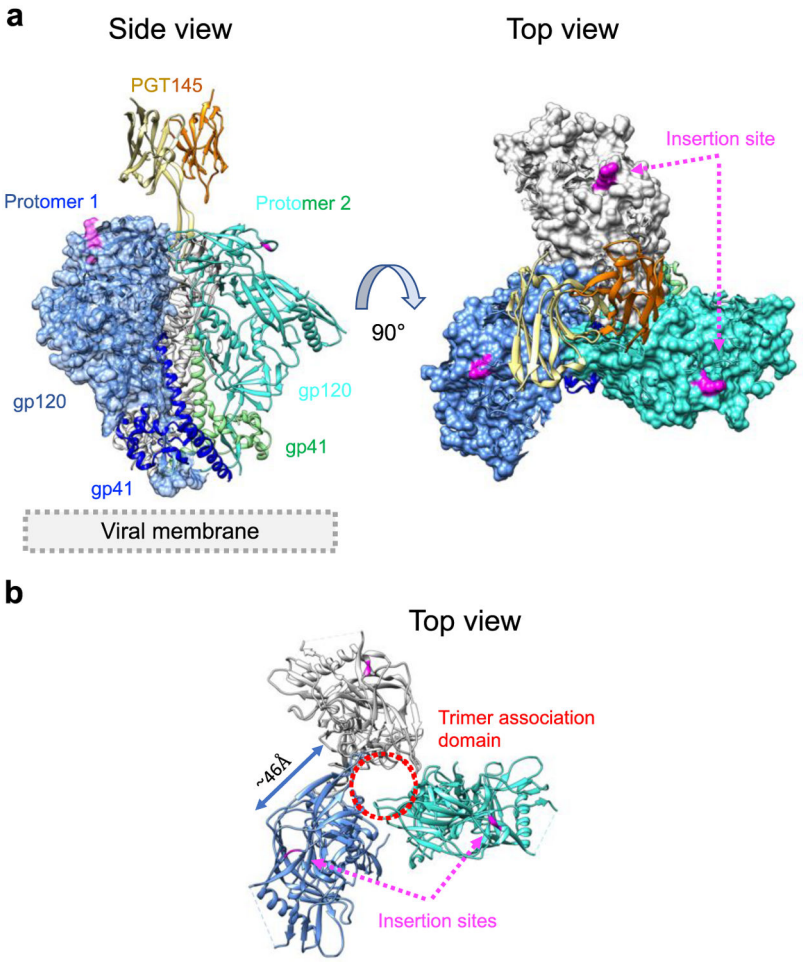

Figure 6.

Spatial mapping the V1 loop insertion and PGT145 binding site. (a) The V1 loop insertion site was mapped on the costructure of BG505 SOSIP in complex with the PGT145 Fab (PDB 5V8L). Each HIV-1 Env trimer contains three protomers of gp120 noncovalently associated with gp41. (left) Protomer 1 is shown in light blue (gp120) and blue (gp41), and visualized using surface representation; protomer 2 is shown in cyan (gp120) and light green (gp41) and displayed using ribbon representation; protomer 3 is shown in gray at the back. The site of V1 loop insertion is shown in magenta. (right) Costructure is shown after rotation 90°, with the orientation from the trimer apex toward the viral membrane, and all protomers are displayed using surface representation. (b) Top view of the gp120 subunit of the three Env promoters that form the Env trimer (the gp41 subunits were removed for visualization). Approximate distance between the PGT145 binding site and the V1 insertion site is specified, and the position of the TAD and the V1 loop insertion site are labeled.